THE JOURNAL OF BIOLOGICAL CHEMISTRY VOL. 284, NO. 8, pp. 5299–5312, February 20, 2009


# Primary Murine Airway Smooth Muscle Cells Exposed to Poly(I,C) or Tunicamycin Synthesize a Leukocyte-adhesive Hyaluronan Matrix*

Received for publication, October 16, 2008, and in revised form, December 12, 2008 Published, JBC Papers in Press, December 16, 2008, DOI 10.1074/jbc.M807965200

**Mark E. Lauer[‡1], Durba Mukhopadhyay[‡1], Csaba Fulop[‡], Carol A. de la Motte[§], Alana K. Majors[§], and Vincent C. Hascall[‡2]**

*From the Departments of [‡]Biomedical Engineering and [§]Pathobiology and Colorectal Surgery, Lerner Research Institute, Cleveland Clinic, Cleveland, Ohio 44195*

**Asthmatic attacks often follow viral infections with subsequent airway smooth muscle cell proliferation and the formation of an abnormal hyaluronan extracellular matrix with infiltrated leukocytes. In this study, we show that murine airway smooth muscle cells (MASM) treated with polyinosinic acid-polycytidylic acid (poly(I,C)), a double-stranded RNA that simulates a viral infection, synthesize an abnormal hyaluronan matrix that binds leukocytes (U937 cells). Synthesis of this matrix is initiated rapidly and accumulates linearly for ~10 h, reaching a plateau level ~7-fold higher than control cultures. MASM cells treated with tunicamycin, to induce endoplasmic reticulum stress, also rapidly initiate synthesis of the abnormal hyaluronan matrix with linear accumulation for ~10 h, but only reach a plateau level ~2-fold higher than control cultures. In contrast to poly(I,C), the response to tunicamycin depends on cell density, with pre-confluent cells producing more abnormal matrix per cell. Furthermore, U937 cell adhesion per hyaluronan content is higher in the sparse matrix produced in response to tunicamycin, suggesting that the structure in the poly(I,C)-induced matrix masks potential binding sites. When MASM cells were exposed to tunicamycin and poly(I,C) at the same time, U937 cell adhesion was partially additive, implying that these two toxins stimulate hyaluronan synthesis through two different pathways. We also characterized the size of hyaluronan produced by MASM cells, in response to poly(I,C) and tunicamycin, and we found that it ranges from 1500 to 4000 kDa, the majority of which was ~4000 kDa and not different in size than hyaluronan made by untreated cells.**

Asthma, a chronic inflammatory disease of the airways (1, 2), is characteristically accompanied by increased airway hyperresponsiveness to various stimuli (such as viruses, allergens, and pollutants) (3–6). Other major features include proliferation of airway smooth muscle cells (7), deposition of an extensive hyaluronan-rich extracellular matrix by these cells into the airway submucosa (8–11), and excessive invasion of the airway mucosa and submucosa by inflammatory cells (mainly T cells of the Th-2 phenotype, eosinophils, macrophages, and mast cells) (12–15).

Hyaluronan is a large glycosaminoglycan in which the disaccharide (glucuronic acid-$\beta$1,3-*N*-acetylglucosamine-$\beta$1,4-) is repeated several thousand times (16). This major constituent of extracellular matrices is generally synthesized by one or more of the three eukaryotic hyaluronan synthases (HAS)[3] (Has1, -2, and -3) (17) at the cytosolic side of the plasma membrane with simultaneous extrusion into the extracellular space. Outside the cell, hyaluronan interacts with both cell surface and extracellular hyaluronan-binding proteins (18), providing the tissue with a structural scaffold. Hyaluronan also has an essential role in many physiological and pathological processes, including cell migration, morphogenesis, tissue regeneration, wound repair, and tumor cell growth and invasion (19). Cells often interact with hyaluronan-based matrices through the cell surface hyaluronan receptor, CD44 (20), which is present in airway smooth muscle cells, both *in vivo* and *in vitro* (21), and is also present on all leukocyte populations (22).

In asthma, the accumulation of excess hyaluronan in the submucosal tissue can lead to severe airway obstruction and death (23). Hyaluronan accumulates in the airway submucosa (24), around the smooth muscle bundles (24), and in the bronchoalveolar lavage fluid (11, 25, 26). A murine bleomycin model by Teder *et al.* (27) has demonstrated that excess amounts of hyaluronan must be removed from the airway submucosa by monocytes/macrophages in a CD44-dependent manner to resolve lung inflammation.

Respiratory viral infections are a major cause of asthma exacerbation and are accompanied by leukocyte infiltration and inflammation of the airways (28, 29). Viral infections account for ~80% of asthma attacks in children (30) and ~70% in adults

* This work was supported, in whole or in part, by National Institutes of Health Grant P11 HL081064 (Pathology of Asthma). The costs of publication of this article were defrayed in part by the payment of page charges. This article must therefore be hereby marked "*advertisement*" in accordance with 18 U.S.C. Section 1734 solely to indicate this fact.

[1] Both authors contributed equally to this work.

[2] To whom correspondence should be addressed: Dept. of Biomedical Engineering/ND20, Cleveland Clinic, Cleveland, OH 44195. Tel.: 216-445-5676; Fax: 216-444-9198; E-mail: hascalv@ccf.org.

[3] The abbreviations used are: HAS, hyaluronan synthase; MASM, murine airway smooth muscle cells; poly(I,C), polyinosinic acid-polycytidylic acid; ER, endoplasmic reticulum; FBS, fetal bovine serum; VCAM-1, vascular cell adhesion molecule 1; KDEL, lysine-aspartate-glutamine-leucine; HMW, high molecular weight; PERK, endoplasmic reticulum resident transmembrane kinase; PKR, double-stranded RNA-dependent protein kinase; DMEM, Dulbecco's modified Eagle's medium; SMC, smooth muscle cell; HABP, hyaluronan binding protein; TEMED, *N,N,N′,N′*-tetramethylethylenediamine; CHAPS, 3-[(3-cholamidopropyl)dimethylammonio]-1-propanesulfonic acid; FACE, fluorophore-assisted carbohydrate electrophoresis; PBS, phosphate-buffered saline.

(31). Rhinovirus was detected by *in situ* hybridization (32) in both bronchial epithelial and underlying submucosal cells in biopsies obtained from the lower airways, and it is likely from the histology that their localization was mesenchymal, namely fibroblasts and/or smooth muscle cells. Furthermore, viral infection in the airway epithelium in asthmatics induces cell death and the desquamation of the epithelial cell layer (33), which then could provide direct viral access to the underlying mesenchymal cells, including the SMCs.

Generally, viruses have two major effects on infected cells. After infection, double-stranded RNA-dependent protein kinase (PKR), a cytosolic and nuclear protein, acts as an intracellular receptor for double strand RNA produced by viral replication. PKR has a key role in limiting viral replication by inactivating the critical translation initiation factor eIF2 by phosphorylation of its $\alpha$ subunit. In the course of a viral infection, large amounts of viral proteins are synthesized and accumulate in the endoplasmic reticulum (ER) (34). Human cytomegalovirus infection has been shown to activate ER resident transmembrane protein kinase (PERK) or PKR-like ER-localized eIF2$\alpha$ kinase, an ER-resident membrane protein that transmits the ER stress signal by phosphorylating eIF-2$\alpha$ at serine 51 (35). This causes translational attenuation and transcriptional up-regulation of genes encoding proteins that facilitate folding or degradation of proteins (35). Thus, PKR and PERK may coordinate to control viral replication.

Both of the above-mentioned pathways of viral infections can trigger SMCs to deposit hyaluronan that is adhesive for leukocytes. For example, human colon SMCs infected with a virus or treated with polyinosinic-polycytidylic acid (poly(I,C)), a double strand RNA that mimics viral genetic material, induce the synthesis of hyaluronan structures that resemble "cables" and readily promote leukocyte adhesion (U937 monocytic cell line) in a CD44-dependent manner (36). Human colon SMCs treated with tunicamycin, or other ER stress inducers, also produce similar adhesive hyaluronan structures. Sections from the colon of patients with inflammatory bowel disease or Crohn disease exhibit abnormal hyaluronan matrices with embedded cells exhibiting ER stress as indicated by KDEL staining (37).

Because the airway inflammation associated with asthma involves the accumulation of a hyaluronan-rich matrix following viral infection, and because viral infection involves ER stress (38), we subjected mouse airway smooth muscle cells (MASM) to a viral mimic (poly(I,C)) and a toxin known to induce ER stress (tunicamycin). Both stressors induced the MASM cells to deposit a hyaluronan-rich extracellular matrix similar to that observed in asthmatic airways. This high molecular weight (~4000 kDa) hyaluronan matrix permitted significant leukocyte adhesion similar to the accumulation of leukocytes in asthmatic airways.

## EXPERIMENTAL PROCEDURES

*Animals and Animal Care*—21-Day-old female BALB/c mice were purchased from Charles River Laboratories (Wilmington, MA) and housed under conditions of constant temperature with 12-h light/dark cycles. Food and water were available *ad libitum*. The mice were sacrificed by administering Nembutal (Ovation Pharmaceuticals, Deerfield, IL) at 0.125 mg/g of mouse weight. All protocols with the animals were approved by the Cleveland Clinic Institutional Animal Care and Use Committee.

*Primary Cell Culture*—After sacrifice, the tracheas were excised and placed in Ham's F-12 nutrient medium with 50 units/ml penicillin, 50 $\mu$g/ml streptomycin, and then maintained at 4 °C on ice. Under a dissecting microscope, the esophagus and surrounding connective tissue were removed. The tracheas were cut longitudinally with a scalpel to expose the lumen and then transferred to 0.15% Pronase (Roche Applied Science) in Ham's F-12 nutrient medium with 50 units/ml penicillin, 50 $\mu$g/ml streptomycin and incubated at 4 °C overnight. The next day, fetal bovine serum (FBS) was added to the tracheas (final concentration 10%) to inhibit further protease degradation. The medium, containing the released cells, was transferred to another tube for isolation of airway epithelial cells for use in a separate study. The tracheas were then brushed with a cotton swab to remove the remaining adherent epithelial cells, cut into small pieces (~30 per trachea), and transferred to a 100-cm$^2$ tissue culture dish for attachment and outgrowth. Approximately 50 $\mu$l of DMEM/F-12 with 100 units/ml penicillin, 100 $\mu$g/ml streptomycin, 0.25 $\mu$g/ml amphotericin B, and 10% FBS was applied to each piece followed by incubation at 37 °C, 5% $CO_2$, and 100% humidity overnight. The next day, 12 ml of the same medium was applied to each 100-cm$^2$ dish that contained the adherent pieces followed by incubation as before. Four days later, SMC outgrowth was apparent, and the residual trachea pieces were removed with forceps. We found that waiting an additional day (5 days total) diminished SMC purity via epithelial outgrowth. The cells were left to multiply for 2 more days, after which they were trypsinized and plated into a 175-cm$^2$ flask. Confluency was reached within about 3–5 days. Typically, we processed 12 tracheas per experiment. Experiments were done on the second passage, which was split 1:2 from the first passage. These cells were positive for the smooth muscle cell marker "caldesmon" as determined by confocal microscopy (C4562, Sigma) (not shown). Additionally, no epithelial contamination was observed by phase-contrast microscopy (not shown). The lack of a suitable marker for myofibroblasts to distinguish them from smooth muscle cells does not permit such a fine distinction, but this is likely to be of minor consequence. For convenience, we refer to these cells as MASM cells.

*Experimental Culture*—For experiments involving poly(I,C) (P0913, Sigma), MASM cells were split 1:2 from passage 1 into 24-well plates. For experiments involving tunicamycin (T7765, Sigma), the splitting ratio was 1:4. The rationale for this approach is described in Fig. 8, and it is related to the observation that the response of the MASM cells to tunicamycin is dependent on cell confluency, whereas the poly(I,C) response is independent of this variable. As a rule, poly(I,C) (10 $\mu$g/ml) and tunicamycin (5 $\mu$g/ml) were applied to the cells 2 days after splitting. The cells were routinely cultured in DMEM/F-12 with 10% FBS, but the FBS content was dropped to 5% for the treatments because a lower serum content facilitates analysis of hyaluronan in the conditioned medium and because Fig. 3 confirms that this change in serum does not affect our other parameters. Treatment duration was 18 h, because our time course studies showed that both tunicamycin and poly(I,C)

induced peak responses for our measured parameters at this time (Figs. 4 and 5). Treatment volume was 0.5 ml per well.

*Leukocyte Adhesion Assay*—Ordinarily, 30 million leukocytes (U937 cells, American Type Tissue Culture, Manassas, VA) were labeled with 100 $\mu$Ci of sodium $^{51}$Cr in 2 ml of RPMI 1640 medium, 50 units/ml penicillin, and 50 $\mu$g/ml streptomycin with 5% FBS for 1 h at 37 °C. Afterward, the leukocytes were washed with 10 ml of washing medium (DMEM/F-12 with 5% FBS, 100 units/ml penicillin, 100 $\mu$g/ml streptomycin, 0.25 $\mu$g/ml amphotericin B, kept at 4 °C) and pelleted at 300 × *g* for 5 min. This washing step was repeated four times. Afterward, the U937 cells were resuspended in 15 ml of washing medium and incubated on ice for 10 min to slow down their metabolism. Three 100-$\mu$l aliquots of the labeled U937 cells were set aside in three separate vials (each containing 200,000 cells) for counting on a scintillation counter to determine counts/min values for a known number of cells. The MASM cells were incubated at 4 °C for 30 min and then gently washed with washing medium one time. The labeled U937 cells were applied to the MASM cells at 1 million per well of a 24-well plate (in 0.5 ml) and incubated at 4 °C for 30 min. Unbound U937 cells were removed by gentle agitation in a circular motion and aspirated. The plates were washed gently two more times. Then half the plate wells were treated with 0.5 turbidity reducing units/ml *Streptomyces* hyaluronidase (100740-1, Seikagaku, East Falmouth, MA) at 0.5 ml/well for 5 min with occasional agitation. The other half of the plate wells were washed two more times. After the 5-min hyaluronidase digestion, the released cells were aspirated, and these wells were washed one more time. The total number of washes for each well was five. The number of leukocytes bound was determined by lysing the cells with 200 $\mu$l of 1% Triton X-100 in distilled water and counting a portion on a scintillation counter.

*Preparation of Hyaluronan for Fluorescent Derivatization with 2-Aminoacridone*—This method (fluorophore-assisted carbohydrate electrophoresis (FACE)) for the quantification of hyaluronan has been partially described elsewhere (39). The conditioned medium (0.5 ml) from each well of a 24-well plate was transferred to a 1.5-ml centrifuge tube containing 50 $\mu$l of proteinase K (25530015, Invitrogen) at 1 mg/ml in 100 mM ammonium acetate, pH 7.0, with 0.01% lauryl sulfate, followed by a 4-h incubation at 60 °C. After removing the medium, each well was washed one time with 0.5 ml of PBS and aspirated, and 0.28 ml of 0.1 mg/ml proteinase K (in 100 mM ammonium acetate, pH 7.0, with 0.001% lauryl sulfate) was applied, followed by 4 h of incubation at 60 °C. The medium samples were then vacuum concentrated and precipitated with (1:4) absolute ethanol at −20 °C overnight. The cell extracts were transferred to 1.5-ml centrifuge tubes and precipitated in the same manner as the medium samples. The precipitates were collected by centrifugation at 13,200 × *g* for 10 min, washed with 1 ml of 75% ethanol at −20 °C, and centrifuged as before. The pellets were air-dried for 20 min and resuspended in 35 $\mu$l of 100 mM ammonium acetate, pH 7.0, for 20 min. The proteinase K was inactivated on a boiling water bath for 5 min. 0.6 $\mu$l of 1% glacial acetic acid was added to each sample, followed by the addition of 0.8 $\mu$l of hyaluronidase SD at 2.5 milliunits/$\mu$l (100741-1A, Seikagaku) and 0.8 $\mu$l of chondroitinase ABC at 25 milliunits/$\mu$l (100330-1A, Seikagaku). The samples were digested at 37 °C overnight and then precipitated overnight with 160 $\mu$l of absolute ethanol at −20 °C. The supernatants were collected by centrifugation at 13,200 × *g* for 10 min. The pellets were washed with 100 $\mu$l of 75% ethanol at −20 °C, and the supernatants were added to the respective first supernatants. The supernatants were lyophilized, resuspended in 25 $\mu$l of 100 mM ammonium acetate, pH 7.0, for 20 min, transferred to a 0.2-ml PCR tube, and lyophilized again. Each lyophilized sample was dissolved in 2 $\mu$l of 2-aminoacridone (A-6289, Invitrogen) (6.25 mM in 42.5% DMSO, 7.5% glacial acetic acid, and 0.625 M sodium cyanoborohydride). The samples were incubated overnight (18 h) at 37 °C. The next day, 0.75 $\mu$l of glycerol was added to each sample, and 2 $\mu$l of this solution was added to each well of a polyacrylamide gel as described below.

*PAGE*—Polyacrylamide gels were cast using mini-Protean II system (Bio-Rad). The gel composition was made of 20% acrylamide (37.5:1, Bio-Rad), 40 mM Tris acetate, pH 7.0, 2.5% glycerol, 10% ammonium persulfate, and 0.1% TEMED). Gels were cast with 0.75-mm spacers and 15-well combs, and the wells were rinsed with electrophoresis running buffer (1× Tris borate/EDTA) by pipetting 150 $\mu$l of the running buffer into the wells six times. The gels were cooled to 4 °C, after which 2 $\mu$l of sample was added to each well. Electrophoresis was accomplished at 300 V (constant voltage) for ~1 h and 20 min. The gel plates were washed with distilled water, and the gels were imaged while in their glass plates.

*Digital Imaging and Data Analysis*—After electrophoresis, the gels (in their glass plates) were placed on a UV transilluminator (Ultra Lum, Claremont, CA) and illuminated at 365 nm. Imaging was done on a Quantix CCD camera (Photometrics, Tucson, AZ), and hyaluronan was quantified using Gel-Pro Analyzer® version 3.0 (Media Cybernetics, Silver Spring, MD). All statistics (Student's *t* tests) were done using KaleidaGraph version 3.6 (Synergy Software, Reading, PA).

*Immunohistochemistry*—MASM cells were fixed in 10% formalin at 4 °C overnight, rinsed with Hanks' balanced salt solution three times, and permeabilized with 0.1% Triton X-100 in pre-cooled Hanks' balanced salt solution at 4 °C for 5 min. Hyaluronan was visualized using confocal microscopy by applying a biotinylated hyaluronan-binding protein (product 385911, EMD Chemicals, Gibbstown, NJ) at 1:100 dilution (5 $\mu$g/ml) in Hanks' balanced salt solution with 1% bovine serum albumin and, subsequently, conjugated to streptavidin, Alexa Fluor® 488 (product S11223, Invitrogen) at 1:500. Mouse monoclonal CD44 (product C7923, Sigma) and KDEL (product SPA-827, StressGen, Victoria, British Columbia, Canada) antibodies were conjugated to Alexa Fluor® 594 secondary antibody (product A21203, Invitrogen).

*Western Blot*—MASM cells were grown to pre-confluency (about 80%) in 6-well plates and treated with tunicamycin or poly(I,C) as described earlier. At the time of harvest, the conditioned medium was removed, and the cells were washed one time in PBS. 0.3 ml of M-PER® mammalian protein extraction reagent (Pierce, 78501) containing Halt™ protease inhibitor mixture (Pierce, 78415) was added to each well and incubated for 5 min at room temperature. The protein extraction was transferred to a 1.5-ml tube, and the protein content was quan-

tified using the Micro BCA™ protein assay kit (Pierce, 23235), yielding about 0.5 mg/ml for each sample. 10 μg of sample protein was added to each well of a 10-well polyacrylamide gel (Invitrogen, NP0321BOX) and blotted to nitrocellulose (Li-Cor, 926-31090, Lincoln, NE). The blot was blocked for 1 h (Li-Cor, 927-40000) and simultaneously probed with antibodies against KDEL at 1:500 (Affinity Bioreagents, PA1-013, Golden, CO) and β-actin at 1:2,000 (Sigma, A5441) in the blocking buffer with 0.1% Tween 20 for 1 h. The blots were washed five times in phosphate-buffered saline with 0.1% Tween 20 and simultaneously probed with IRDYE secondary antibodies (Li-Cor, 926-32211 and 926-32222) at 1:15,000 dilution in blocking buffer with 0.1% Tween 20 and 0.01% lauryl sulfate for 45 min. The blots were washed as before and imaged on an Odyssey infrared imaging system (Li-Cor).

*Size Determination of Hyaluronan*—Pre-confluent (~90%) MASM cells, cultured in 175-cm$^2$ flasks, were incubated with poly(I,C) (10 μg/ml), tunicamycin (5 μg/ml) or untreated for 18 h as described under "Experimental Culture." Afterward, the cells were rinsed two times with 25 ml of room temperature PBS and digested with 8 ml of proteinase K (25530015, Invitrogen) at 0.1 mg/ml in 100 mM ammonium acetate, pH 7.0, with 0.01% lauryl sulfate, followed by a 4-h incubation at 60 °C with occasional (every 30 min) agitation of the flasks to ensure all surface area was covered by the digesting solution. The extracts were transferred to 40-ml centrifuge tubes and precipitated with 32 ml of absolute ethanol at −20 °C overnight. The samples were centrifuged at 13,200 × *g* for 20 min (4 °C), discarding the supernatant. The samples were washed with 40 ml of 75% absolute ethanol (−20 °C) and centrifuged as before. The pellet was allowed to air-dry at room temperature for 1 h and resuspended in 1 ml of 100 mM ammonium acetate, pH 7.0, for an additional hour. Residual proteinase K was heat-inactivated by applying the samples to a boiling water bath for 10 min. After a brief spin (1 min, 13,200 × *g*), the samples were transferred to 1.5-ml centrifuge tubes, (using a 9-inch Pasteur pipette) and vacuum concentrated to 100 μl. DNase (3 μl at 2 units/μl, 2224, Ambion, Austin, TX) and RNase (3 μl at 1.28 μg/μl, 109169, Roche Applied Science) were added to the samples and incubated at 37 °C overnight followed by precipitation with 4 volumes of absolute ethanol at −20 °C overnight. The samples were centrifuged for 10 min at 4 °C and 13,200 × *g*, discarding the supernatant. The pellets were washed with 500 μl of 75% ethanol (−20 °C), centrifuged as before, and permitted to air dry for 20 min. The pellet was resuspended in 19 μl of 100 mM ammonium acetate, pH 7.0, for 20 min and placed on a boiling water bath for 5 min to inactivate the DNase and RNase enzymes. A-(2→3,6,8,9)-Neuraminidase (1 μl at 0.005 unit/μl, N8271, Sigma) was added to each of the samples to degrade sialic acid containing mucin oligosaccharides. For some experiments, the samples were divided into halves (10 μl each), and the hyaluronan was digested with *Streptomyces* hyaluronidase (1 μl at 0.2 turbidity reducing unit/μl) to confirm the purity of hyaluronan on the agarose gel. These digests were incubated at 37 °C overnight, inactivating the enzymes on a boiling water bath the next day for 5 min. The samples were lyophilized and resuspended with Tris acetate/EDTA (TAE; 4 mM Tris, 50 mM EDTA, pH 8.26) in the same volume as in the previous digests (either 10 or 20 μl). These samples were analyzed on 1% agarose gels (50041, SeaKem HGT, Cambrex, Walkersville, MD) that were pre-run at 80 V (constant) for 6 h to remove impurities, using TAE as the electrophoresis buffer. Loading buffer (0.2% bromphenol blue in 85% glycerol; 2 μl for each 10-μl sample) was added to each sample, followed by electrophoresis at 100 V for 1 h and 11 min (0.5 cm thick, 11 × 8-cm gel). Hyaluronan molecular weight standards were also used in this analysis (Select-HA™ LoLadder, HiLadder, and Mega-HA™ Ladder; Hyalose, Oklahoma City, OK). Afterward, the gels were equilibrated in 200 ml of 30% ethanol with gentle shaking (~60 rpm) for 1 h and stained with Stains-All (200 ml at 6.25 μg/ml in 30% ethanol; E-9379, Sigma) overnight in darkness. The next day, the stain was discarded, and the gels were rinsed with distilled water, exposing them to light for ~25 min until background was minimal. The gels were imaged on a light box with a standard, color, digital camera.

## RESULTS

*Leukocytes Bind Hyaluronan Cables Produced by MASM Cells Stimulated with the Viral Mimic Poly(I,C)*—Under routine conditions (Fig. 1, *A–C*), cultured MASM cells are coated with small amounts of hyaluronan (*B, green*) on the apical surface that is not adhesive for leukocytes. MASM cells treated with poly(I,C) (Fig. 1, *D–F*) synthesize an abnormal hyaluronan matrix (*E, green*), which has been described previously as resembling cables (36). U937 leukocytes, stained with an antiserum for human CD44 that does not interact with murine CD44 (Fig. 1*D, red*), adhere to this matrix. The following experiments define processes by which MASM cells initiate synthesis of the hyaluronan matrices with structural information that promotes leukocyte adhesion and subsequent degradation of the abnormal matrix.

MASM cells were cultured for 18 h in 5% FBS with different concentrations of poly(I,C) (0–50 μg/ml). Fig. 2*A* shows increased accumulation of hyaluronan in the cell layer at 1 μg/ml poly(I,C) with a further increase to a plateau level ~4-fold above the control (without poly(I,C)) in 10 μg/ml poly(I,C) ($p < 0.0001$). Fig. 2*B* shows that the adhesion of U937 leukocytes (4 °C, 30 min) increased to a plateau level at 1 μg/ml poly(I,C) ($p < 0.002$), and that the majority of U937 leukocytes, in parallel cultures, was released by a brief digestion with *Streptomyces* hyaluronidase, specific for hyaluronan. The results indicate that poly(I,C) induces the synthesis of a hyaluronan matrix in the cell layer that is adhesive for leukocytes. At 1 μg/ml poly(I,C), the amount of leukocyte adhesion was not directly related to the amount of hyaluronan cable production (40.7% of the maximum). Most likely, this is related to the availability of hyaluronan in which the surface area available for leukocyte adhesion becomes masked as more and more hyaluronan accumulates (as further described in Fig. 8). A concentration of 10 μg/ml poly(I,C) was used in the subsequent experiments.

*A Serum Factor Is Necessary for Poly(I,C) to Induce Hyaluronan Production and Hyaluronan-mediated Leukocyte Adhesion to MASM Cells*—MASM cell cultures were treated for 18 h with (Fig. 3*A*) or without (Fig. 3*B*) 10 μg/ml poly(I,C) and with increasing concentrations of FBS (0–10%). In the presence of

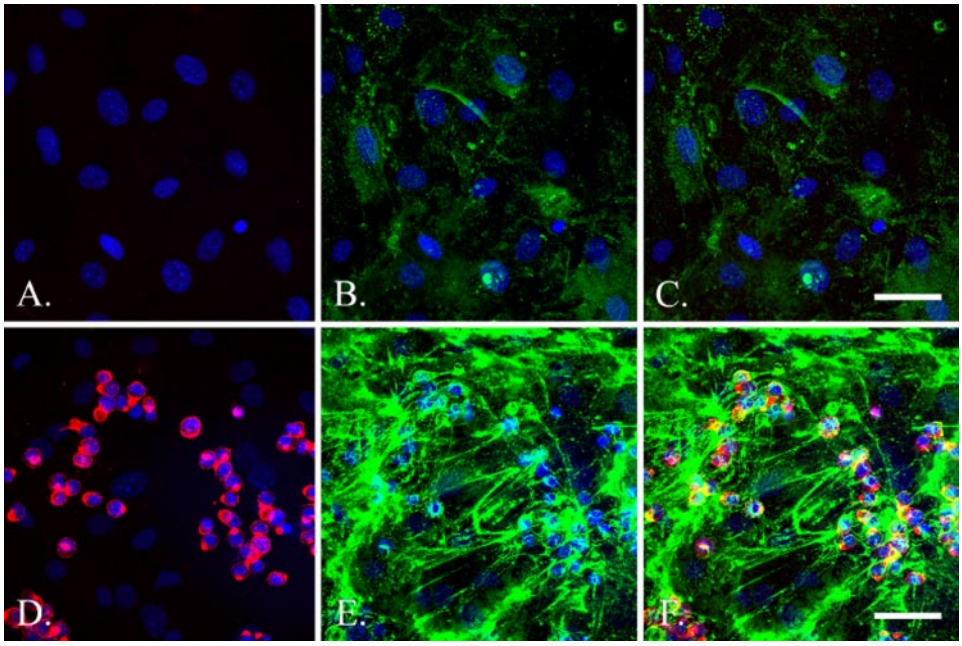


FIGURE 1. **MASM cells produce hyaluronan "cable" structures that promote leukocyte adhesion in response to poly(I,C).** MASM cells were treated with (*D–F*) or without (*A–C*), poly(I,C), followed by the application of U937 leukocytes. The nontreated MASM cells do not promote leukocyte adhesion via the small amount of hyaluronan on their apical surface (*B, green*). In contrast, poly(I,C) induced synthesis of hyaluronan (*E, green*). U937 leukocytes bind to the hyaluronan produced in response to poly(I,C) (*D, red*) but are absent in the untreated culture (*A*). The leukocytes are stained with a human-specific anti-CD44 antibody that binds to the human-derived U937 cells but not the underlying MASM cells. 4′,6-Diamidino-2-phenylindole-stained nuclei are *blue*. The merged views are in *C* and *F*, and their *white bars* indicate 50-$\mu$m magnification. This experiment was repeated >3 times with different experiments.

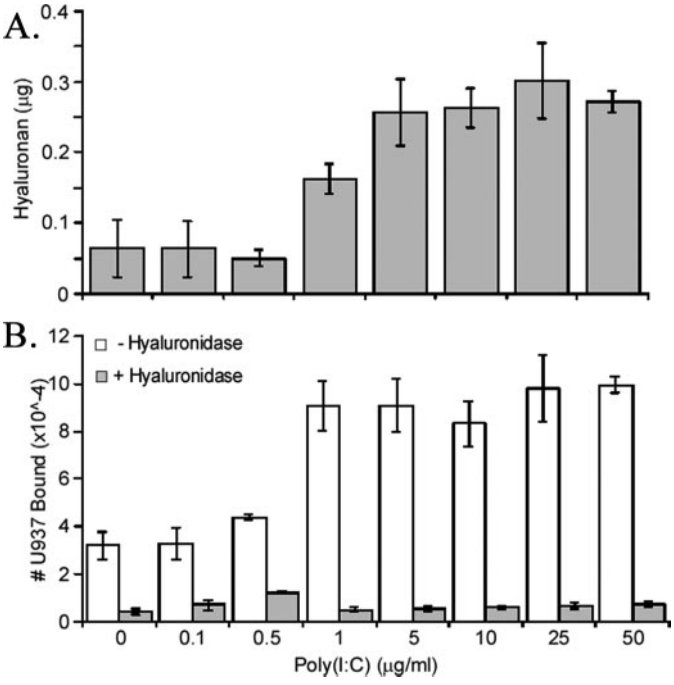


FIGURE 2. **Dose relationship of poly(I,C) to the hyaluronan production and hyaluronan-mediated leukocyte adhesion of MASM cells.** *A* shows the FACE analyses of hyaluronan for the cell matrix of MASM cells treated with different doses of poly(I,C) in 5% FBS ($n = 6$). *B* shows the number of U937 leukocytes bound (*white bars*) to the MASM cells for this same experiment compared with the number of leukocytes remaining after release by treatment with *Streptomyces* hyaluronidase (5 min, 4 °C) (*gray bars*) ($n = 3$). *Error bars* represent standard deviation.

poly(I,C), the hyaluronan content increased in the cell layer with increasing concentrations of FBS (Fig. 3*A*, *white bars*) but remained constant in the medium fractions (Fig. 3*A*, *gray bars*). In the absence of poly(I,C), hyaluronan secreted into the medium fractions remained nearly constant (15.2 ± 1.6 $\mu$g/culture) with increasing FBS (Fig. 3*B*, *gray bars*) and close to the amounts secreted into the medium fractions in poly(I,C)-treated cultures (21.4 ± 2.3 $\mu$g/culture). In contrast, for each FBS concentration, the amounts of hyaluronan in the cell layers (Fig. 3*B*, *white bars*) were much lower when untreated than for the poly(I,C)-treated cultures.

Adhesion of leukocytes (4 °C, 30 min) was measured in parallel cultures treated with (Fig. 3*C*, *white bars*) or without (Fig. 3*D*, *white bars*) poly(I,C). Replicate cultures in each case were treated with *Streptomyces* hyaluronidase to determine hyaluronan-mediated leukocyte adhesion (Fig. 3, *C* and *D*, *gray bars*). Poly(I,C) treatment in the absence of FBS showed a significant ($p < 0.002$) hyaluronan-mediated leukocyte adhesion that increased further at 0.5% FBS (Fig. 3*C*, *white bars* compared with *gray bars*). Residual *Streptomyces* hyaluronidase independent leukocyte adhesion was highest in the culture without FBS and decreased with increasing FBS, reaching a minimum at 5% FBS (Fig. 3*C*, *gray bars*). The cultures without poly(I,C) treatment showed a small proportion of hyaluronan-mediated leukocyte binding, which was essentially independent of FBS concentration (Fig. 3*D*, *white bars* compared with *gray bars*). Hyaluronan-mediated adhesion was determined from the data in Fig. 3, *C* and *D*, by subtracting the values for the hyaluronidase residual bound leukocytes from the total bound (*white bars* minus *gray bars*), and the results are plotted in Fig. 3*E*. The values for poly(I,C)-treated cultures in the presence of 0.5% and higher FBS were up to 10-fold higher ($p < 0.003$) than the values in the untreated cultures.

The results in Fig. 3 indicate that poly(I,C) increases hyaluronan contents of the cell layer and hyaluronan-mediated leukocyte adhesion even in the absence of FBS, but that the presence of FBS increases the response. For comparison, in cultures without FBS, the ratio of hyaluronan in the cell layer to that in the medium was 2.8, whereas the ratio was 8.5 in cultures with 5% FBS (Fig. 3*A*, *arrows*). In contrast, the amount of hyaluronan secreted into the medium compartment was independent of FBS concentration. Thus, the increase in hyaluronan in the cell layer in response to poly(I,C) is independent of the pathway that is involved in hyaluronan secretion. Based on the results showing that the hyaluronan response in the poly(I,C)-treated cultures relative to the untreated cultures was at a plateau level in

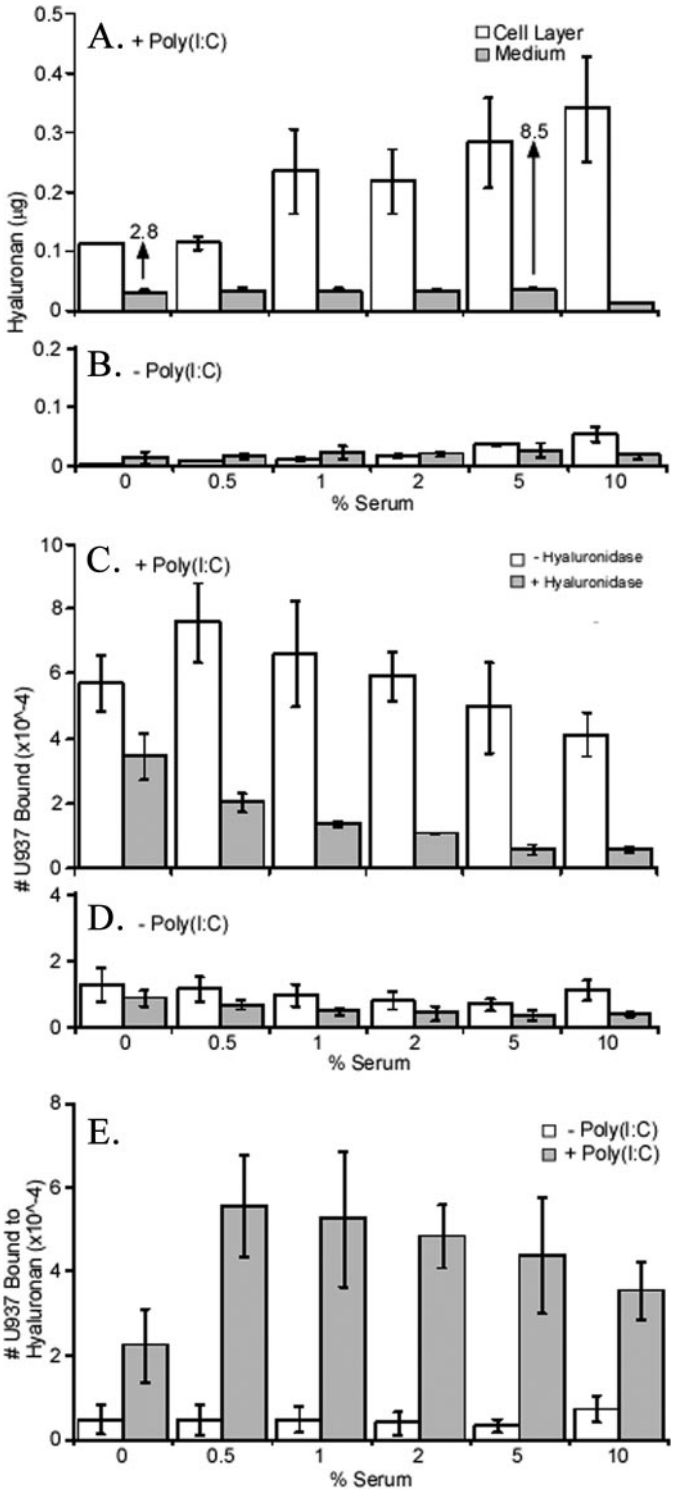


FIGURE 3. **Relation of serum to poly(I,C)-induced hyaluronan production and hyaluronan-mediated leukocyte adhesion of MASM cells.** *A* shows the FACE analyses of hyaluronan for MASM cells treated with 10 $\mu$g/ml poly(I,C) and different doses of FBS in the cell layer (*white bars*) and secreted into the medium (*gray bars*) ($n = 2$). *B* shows the effect of FBS dosage on MASM cells that were not treated with poly(I,C) ($n = 2$). *C* and *D* show the number of U937 leukocytes bound (*white bars*) to poly(I,C)-treated (*C*) or nontreated (*D*) MASM cells for this same experiment compared with the number of leukocytes remaining after release by hyaluronan degradation (*gray bars*) ($n = 3$). *E* shows data from *C* and *D* expressed as the number of leukocytes bound directly to hyaluronan on poly(I,C)-treated (*gray bars*) and nontreated (*white bars*) MASM cells ($n = 3$). *Error bars* represent standard deviation for $n = 3$ or range for $n = 2$.

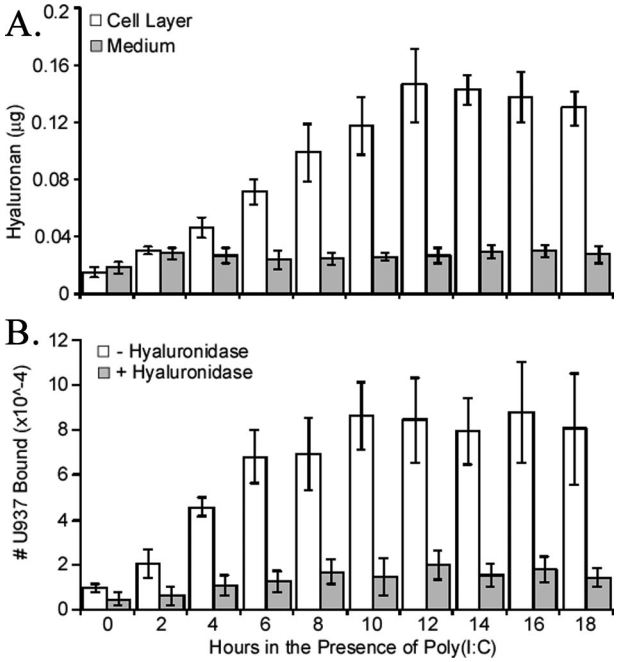


FIGURE 4. **Poly(I,C) kinetics of hyaluronan production and hyaluronan-mediated leukocyte adhesion by MASM cells.** *A* shows the FACE analyses of hyaluronan for MASM cells treated with 10 $\mu$g/ml poly(I,C) and 5% FBS for different times. Hyaluronan present in the cell layer is shown as *white bars*, and the amount secreted into the medium is shown as *gray bars* ($n = 4$). *B* shows the number of leukocytes bound (*white bars*) to poly(I,C)-treated MASM cells for this same experiment compared with the number of leukocytes remaining after release by hyaluronidase (*gray bars*) ($n = 4$). *Error bars* represent standard deviation.

the cell layer at 5% FBS with minimal non-hyaluronan-mediated leukocyte adhesion, this concentration of FBS was used in the following experiments.

*Differential Hyaluronan Kinetics of Poly(I,C) and Tunicamycin Stimulation of MASM Cells*—Fig. 4 shows the results of an experiment to determine the time course of the poly(I,C) response. All cultures were started at time 0 in the presence of 5% FBS, and a small aliquot of poly(I,C) was added at different times during the 18-h incubation to yield a final concentration of 10 $\mu$g/ml. Controls (Fig. 4, *A* and *B*, *bars at time 0*) were incubated without poly(I,C) for the entire 18 h. Exposure of the MASM cells to poly(I,C) for 2 h already showed an increase in the amount of hyaluronan in the cell layer, with a nearly linear increase with time up to 12 h of exposure, reaching a plateau value 9.9-fold ($p < 0.0001$) over the 0 exposure control cultures (Fig. 4*A*, *white bars*). The amounts of hyaluronan recovered in the medium fractions were the same for all times, except for the control (time 0), which was 31% lower than the average value for all of the treated cultures (Fig. 4*A*, *gray bars*). This confirmed that hyaluronan secretion in the medium is not dependent on poly(I,C) treatment. The results for the hyaluronan in the cell layer were essentially the same for a time course experiment in which the poly(I,C) was added to all cultures at time 0 and then stopped at different times up to 18 h (data not shown). Fig. 4*B* shows the U937 leukocyte adhesion for parallel cultures exposed to 10 $\mu$g/ml poly(I,C) for different times. Hyaluronan-mediated leukocyte adhesion already increased at the 2-h time point, with a nearly linear increase to a plateau value ($p < 0.0003$) at about 10 h, similar to the increase in hyaluronan in

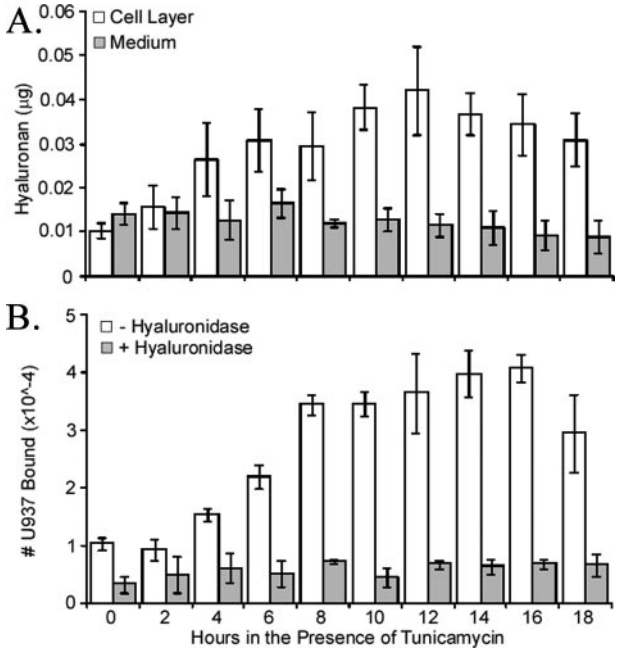


FIGURE 5. **Tunicamycin kinetics of hyaluronan production and hyaluronan-mediated leukocyte adhesion by MASM cells.** *A* shows the FACE analyses of hyaluronan for MASM cells treated with 5 μg/ml tunicamycin for the same times (and using the same original cell preparation) presented in Fig. 4. Hyaluronan derived from the cell layer is shown as *white bars*, and the amounts of hyaluronan secreted into the medium are shown as *gray bars* ($n = 4$; *error bars* represent standard deviation). *B* shows the number of leukocytes bound (*white bars*) to tunicamycin-treated MASM cells for this same experiment compared with the number of leukocytes remaining after release by hyaluronan degradation (*gray bars*) ($n = 2$; *error bars* represent range).

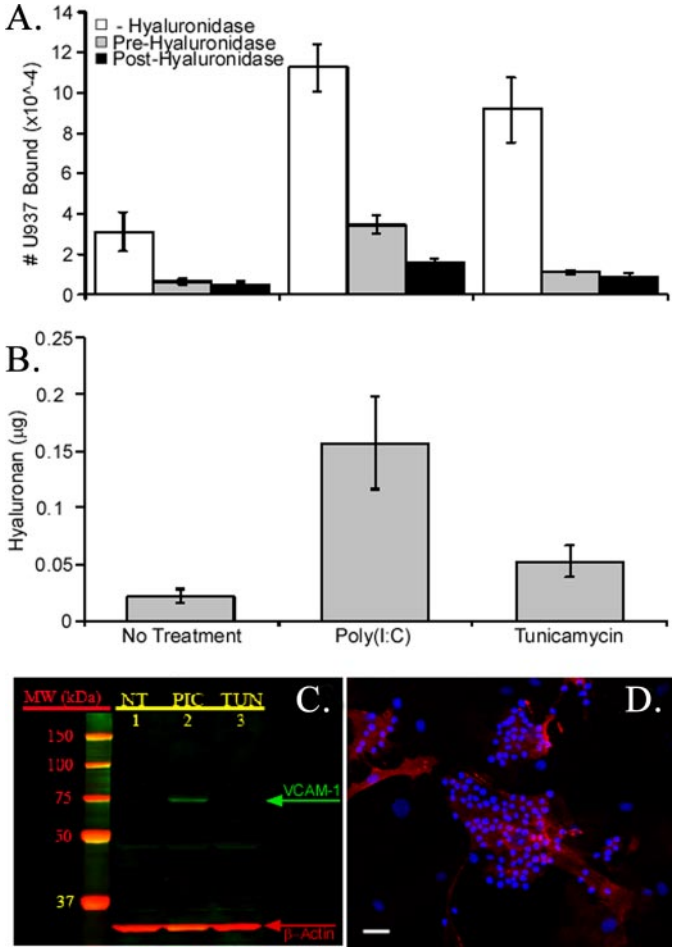


FIGURE 6. **Hyaluronan-dependent and -independent mediated leukocyte adhesion to MASM cells treated with poly(I,C) and tunicamycin and its relation to VCAM-1.** *A* shows the number of leukocytes bound to nontreated, poly(I,C)-treated, or tunicamycin-treated MASM cells (*white bars*) compared with the number of leukocytes bound to MASM cells that had the hyaluronan removed from the MASM cells before application of the leukocytes (*gray bars*), or released after binding by hyaluronan degradation (*black bars*) ($n = 4$). *B* shows the hyaluronan results of FACE analysis for the MASM cells comparing the three treatment groups ($n = 4$). *Error bars* represent standard deviation. *C* shows a Western blot of MASM cell extracts from cells treated with poly(I,C) (*PIC*; *lane 2*), tunicamycin (*TUN*; *lane 3*), or untreated (*NT*; *lane 1*). The blots were probed with an antibody against VCAM-1 (*green*; *lanes 1–3*) and an antibody against β-actin (*red*; *lanes 1–3*) as a loading control. Molecular weight standards are shown as a *red ladder*. This blot was repeated three times with three different samples with essentially identical results. *D* shows U937 cells (*small blue nuclei*) congregating on poly(I,C) MASM cells (*larger blue nuclei*) that had been pretreated with *Streptomyces* hyaluronidase. The U937 cells adhered to MASM cells that were highly expressing VCAM-1 (*red*). *Magnification bar* is 100 μm.

the cell layer. The results in Fig. 4 show that the synthesis of the hyaluronan matrix that is adhesive for leukocytes is initiated rapidly upon exposure to poly(I,C) and that it continues to increase with linear kinetics for 10–12 h before stopping.

Tunicamycin at a plateau concentration of 5 μg/ml induced synthesis of an adhesive hyaluronan matrix by MASM cells cultured for 18 h in the presence of 5% FBS (data not shown). Fig. 5 shows hyaluronan production and leukocyte adhesion for cultures treated with 5 μg/ml tunicamycin and 5% FBS for different times up to 18 h. Similar to the poly(I,C) time course, synthesis of the hyaluronan in the cell layer was initiated rapidly and increased linearly with time before reaching a plateau ($p < 0.0002$) between 10 and 12 h (Fig. 5*A*, *white bars*). In contrast to the poly(I,C)-treated cultures, the hyaluronan content in the cell layer at plateau was much less (25.2 ± 1.7 μg/culture (Fig. 5*A*) *versus* 111.3 ± 8.1 μg/culture (Fig. 4*A*); $p < 0.0001$). The amounts secreted into the medium compartment showed a tendency to decrease with time, particularly after 8 h of treatment (Fig. 5*A*, *gray bars*). As for the poly(I,C) treatment, tunicamycin treatment initiates an independent mechanism for formation of the hyaluronan matrix in the cell layer compared with that for secretion into the medium. Fig. 5*B* shows the adhesion of U937 leukocytes for parallel cultures. In this case, the adhesion showed a lag of 2–4 h before increasing to a maximum plateau value ($p < 0.0001$) at 8–12 h of tunicamycin treatment. Interestingly, the number of leukocytes bound per increase in cell layer hyaluronan content is much higher ($p < 0.0001$) for the maximum plateau values for tunicamycin treatment than for the poly(I,C) treatment (~120 *versus* 55 leukocytes/μg of hyaluronan, respectively) as is discussed below.

*Selective Induction of MASM Cell Adhesion Molecules by Poly(I,C), but Not Tunicamycin, Despite Similar Hyaluronan-mediated Leukocyte Adhesion*—Fig. 6 shows an example in which the hyaluronan synthesis and leukocyte adhesion parameters are compared for identical MASM cell cultures treated with poly(I,C) (10 μg/ml) and tunicamycin (5 μg/ml) under standard conditions (5% FBS, 18 h). In this case, at the end of the 18-h incubation, some cultures were treated with *Streptomyces* hyaluronidase before testing them for leukocyte adhesion (*Pre-Hyaluronidase, gray bars*) and others after leukocyte adhesion (*Post-Hyaluronidase, black bars*) (Fig. 6*A*). The control cultures

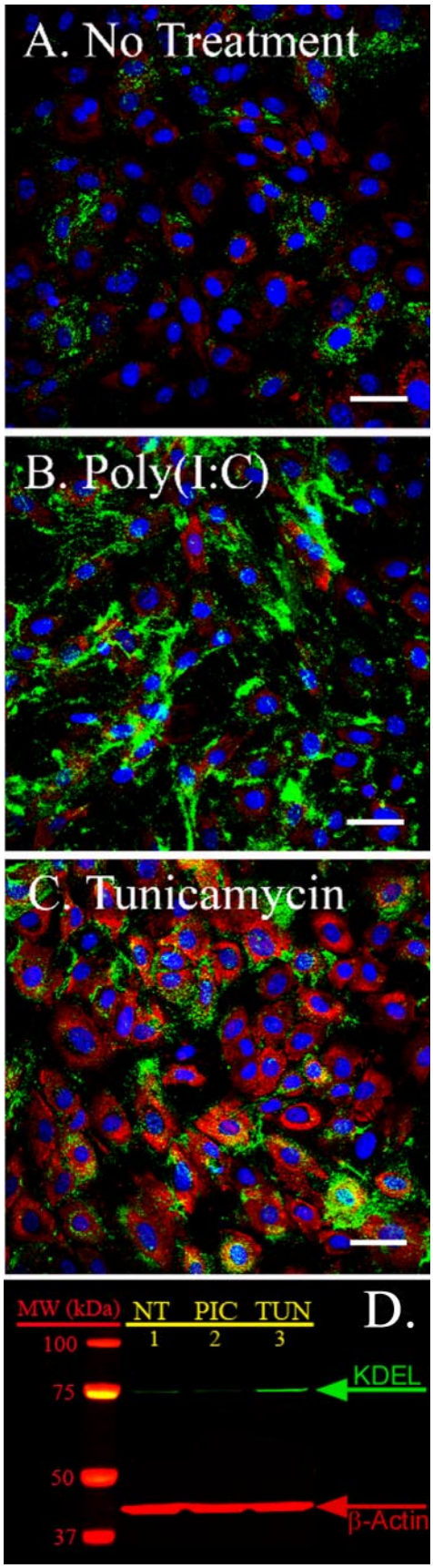


FIGURE 7. **Tunicamycin, but not poly(I,C), induces endoplasmic reticulum stress.** MASM cells were either nontreated (*A*), treated with poly(I,C) (*B*), or treated with tunicamycin (*C*) and probed for hyaluronan (*green*) and KDEL (*red*) (nuclei are *blue*). Although both tunicamycin and poly(I,C) induced the accumulation of hyaluronan on the cell surface when compared with the nontreated cells, tunicamycin induced the expression of KDEL-containing proteins (indicative of an unfolded protein response), whereas poly(I,C) failed to induce its expression (40×) (*magnification bar* is 50 μm). *D* shows a Western blot in which MASM cell protein extracts were probed for KDEL (*green*) and β-actin as a loading control (*red*) to confirm our confocal observations (*A–C*). *Lanes 1–3* represent MASM cells untreated (*NT*; *lane 1*), or treated with poly(I,C) (*PIC*; *lane 2*) or tunicamycin (*TUN*; *lane 3*). Molecular weight standards are shown as *red/yellow*. This blot was repeated three times with three different samples with essentially identical results.

(Fig. 6*A*, *No Treatment*) showed some hyaluronan-mediated adhesion of the leukocytes (*white bar* compared with *black bar*). The poly(I,C) and tunicamycin cultures showed 3.6- and 2.9-fold ($p < 0.0001$ and 0.0008, respectively) increases in hyaluronan-mediated leukocyte adhesion compared with no treatment (Fig. 6*A*, *white bars*), respectively. Interestingly, pretreatment of poly(I,C) cultures with hyaluronidase showed a significant ($p < 0.0004$) increase in the number of leukocytes bound compared with the number that remained bound when the hyaluronidase treatment was done after leukocyte adhesion (Fig. 6*A*, *gray bar* compared with *black bar*), and both were significantly ($p < 0.0001$ and 0.0004, respectively) higher than the respective control cultures. This is likely because of up-regulation of VCAM on the MASM cells, which permits adhesion through interaction with VLA4 integrin on the leukocytes (36). We observed that poly(I,C), but not tunicamycin, induces VCAM-1 synthesis by the MASM cells (Fig. 6*C*). Additionally, we found that poly(I,C)-treated MASM cells pretreated with *Streptomyces* hyaluronidase promote U937 cell adhesion to cells expressing high levels of VCAM-1 (Fig. 6*D*). The presence of the hyaluronan matrix during the leukocyte adhesion step masks about half of the sites that are exposed when the hyaluronan matrix is removed prior to leukocyte binding. Notably, the tunicamycin-treated cultures do not show a significant difference between hyaluronidase treatments before and after leukocyte adhesion and only a modest increase relative to the control cultures. This is consistent with ER stress, which drastically inhibits new protein synthesis except for select proteins, such as chaperones, in an attempt to facilitate proper folding of proteins in the endoplasmic reticulum.

In contrast to the similarity of the leukocyte adhesion response, the increase in hyaluronan deposition in the matrix of the tunicamycin-treated MASM cells was much less ($p < 0.003$) than for the poly(I,C)-treated cells (Fig. 6*B*). Typically, tunicamycin increases hyaluronan deposition less than 2-fold, whereas poly(I,C) yields 7-fold or greater increases. The observation that similar numbers of leukocytes bind to the hyaluronan matrix in both treatments (Fig. 6*A*) suggests that the organization of the newly synthesized matrix may be much more dispersed in the tunicamycin-treated cultures, with less masking of potential binding sites, than for poly(I,C)-treated cultures.

*Despite Similar Hyaluronan-mediated Leukocyte Adhesion by MASM Cells Stimulated with Poly(I,C) and Tunicamycin, Only the Tunicamycin Response Is Associated with the Up-regulation of ER Chaperones*—Fig. 7, *A–C,* shows confocal micrographs of control, poly(I,C), and tunicamycin cultures stained for hyaluronan (*green*) and KDEL (*red*), a peptide sequence marker for chaperones synthesized in response to ER stress. The KDEL reaction for the tunicamycin culture is much stron-

ger than for the poly(I,C) and control cultures, consistent with the lack of an ER stress response to the poly(I,C) treatment. This was verified by Western analyses of cell extracts (Fig. 7*D*), which showed a significant increase in the expression of a KDEL-containing protein from the extract of the tunicamycin-treated culture, but not in the control or poly(I,C) extracts. The molecular mass of this protein is near 74 kDa, and its identity is probably GRP78 (glucose-regulated protein 78). As expected from the hyaluronan analyses in Fig. 6*B*, the poly(I,C) culture showed a more extensive hyaluronan response than the tunicamycin-treated cultures, and both were increased relative to the control culture (Fig. 7, *A–C*, *green*).

*In Contrast to Poly(I,C), the Response of MASM Cells to Tunicamycin Is Dependent on Confluency*—Whereas the hyaluronan content and leukocyte adhesion to MASM cells in response to poly(I,C) was consistent from culture-to-culture, we observed some variation from experiment-to-experiment with these parameters when the MASM cells were treated with tunicamycin. We began to suspect that cell density might be the cause of this variation and examined this parameter in detail (Fig. 8). Hyaluronan in the matrices of the control (no treatment) and the poly(I,C)-treated cultures increased in proportion to the cell density, with the poly(I,C) showing large (7–10-fold; $p < 0.002–0.0002$) increases over control levels (Fig. 8*A*, note that the scale for the control and tunicamycin cultures are expanded three times for comparison). In contrast, the hyaluronan contents in the matrices of the tunicamycin-treated cells were nearly independent ($p > 0.4–0.8$) of cell density. Thus, at the pre-confluent density, tunicamycin stimulated a 58% increase ($p < 0.008$) in matrix hyaluronan relative to the control (Fig. 8*A*, *white bar above dashed line*), whereas at the post-confluent density, there was no difference with its control ($p > 0.08$).

Fig. 8*B* shows hyaluronan-mediated leukocyte adhesion (the difference between cultures with adherent leukocytes before and after hyaluronidase treatment) for this experiment. Control cultures at the pre-confluent density showed some hyaluronan-mediated leukocyte adhesion, whereas those at confluency and post-confluency did not. Poly(I,C) cultures showed similar ($p > 0.2–0.4$) leukocyte binding levels at all confluencies (Fig. 8*B*). In contrast, hyaluronan levels in the cell layer of poly(I,C)-treated cultures increased proportional to cell number (Fig. 8*A*) such that the number of leukocytes bound per increase in hyaluronan decreased with increasing cell density, from ~460 U937/$\mu$g hyaluronan at pre-confluency to ~170 U937/$\mu$g hyaluronan at post-confluency. This again suggests that increased hyaluronan matrix deposition in poly(I,C)-treated cultures masks potential binding sites. For tunicamycin-treated cultures, leukocyte adhesion decreased with increasing cell density, with a high level equivalent to poly(I,C) at pre-confluency decreasing to 29% at post-confluency (Fig. 8*B*). In this case, the decrease in leukocyte adhesion correlated more closely with the decrease in the amount of tunicamycin-induced additional hyaluronan in the matrix (Fig. 8*A*, areas above the *dashed lines*), such that the number of leukocytes bound per increase in hyaluronan matrix deposition remained nearly the same, between ~2100 U937/$\mu$g hyaluronan at pre-confluency and ~1700 U937/$\mu$g hyaluronan at post-confluency. The tunicamycin results suggest that the MASM cells in higher density cultures might not be as active in protein synthesis as in low density cultures and hence less sensitive to the ER-stress induced by tunicamycin.

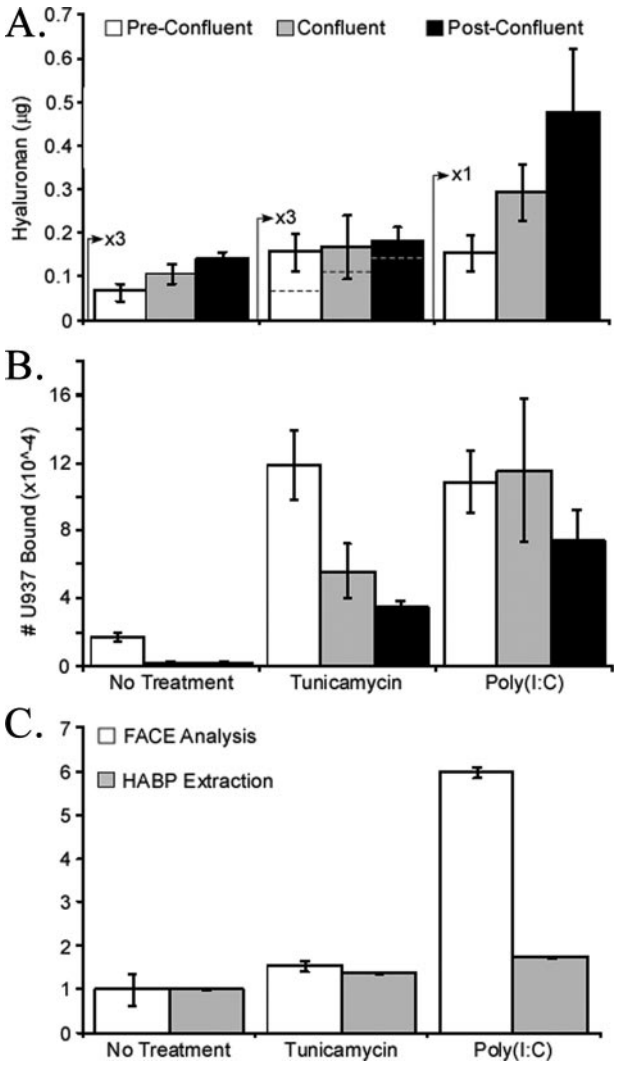


FIGURE 8. **MASM cell confluency and its differential effect on tunicamycin and poly(I,C)-induced hyaluronan masking.** *A* shows the FACE analysis of hyaluronan for MASM cells plated at pre-confluency (*white bars*), confluency (*gray bars*), and post-confluency (*black bars*) ($n = 4$). The data for the non-treated cells and the tunicamycin-treated cells were multiplied ×3 for better visualization. *B* shows the number of leukocytes bound via hyaluronan to the MASM cells for this same experiment ($n = 3$). *C* contrasts hyaluronan measurement from MASM cells using a fluorescent-tagged HABP (which measures the amount of available hyaluronan surface area) with FACE analysis (which gives the total hyaluronan mass) presenting the data as fold increase above untreated. *Error bars* represent standard deviation.

Because the data imply that the poly(I,C)-induced hyaluronan matrix masks potential binding sites, we applied a fluorescent-tagged biotinylated hyaluronan-binding protein (HABP) to the poly(I,C)-treated MASM cells, with the rationale that the probe would give an estimate of the amount of hyaluronan surface area available. This was accomplished by extracting the bound HABP with *Streptomyces* hyaluronidase and counting the extract on a fluorometer. These values were compared with values representative of the total hyaluronan mass (by FACE analysis), which was performed on parallel cultures (Fig. 8*C*). The amount of hyaluronan, determined by HABP extraction (*gray bars*), was similar (although statistically different; $p < 0.0001$) for MASM cells treated with tunicamycin and poly(I,C), both of which gave a mod-

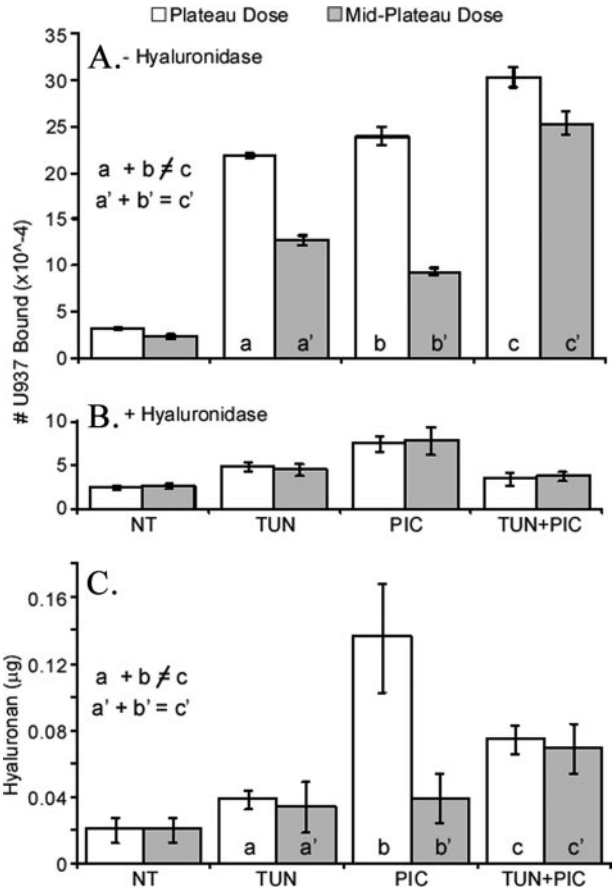


FIGURE 9. **Poly(I,C) and tunicamycin induce hyaluronan synthesis and hyaluronan-mediated leukocyte adhesion by complementary, yet independent, pathways.** MASM cells were either untreated (*NT*) or treated with poly(I,C) (*PIC*), tunicamycin (*TUN*), or a combination of both (*TUN*+*PIC*). These treatments were made at doses that were known to induce a maximum plateau response (*white bars*) for the leukocyte adhesion assay (10 and 5 $\mu$g/ml for poly(I,C) and tunicamycin, respectively) and a mid-plateau dose (*gray bars*) that gave leukocyte adhesion values that were about 50% of the maximum value (0.1 and 0.5 $\mu$g/ml for poly(I,C) and tunicamycin, respectively). *A* shows the number of leukocytes bound to the MASM cells under these conditions. *B* shows the number of leukocytes remaining after treatment with *Streptomyces* hyaluronidase. *C* presents the hyaluronan mass (by FACE analyses) of hyaluronan from the cell matrices for the same experiment. *Error bars* represent standard deviation.

est (27 and 42%, respectively) increase relative to the untreated control. In contrast, FACE analysis showed a similar fold increase with respect to the HABP extraction ($p > 0.03$) for the tunicamycin-treated cells while showing a 3.4-fold increase ($p < 0.0001$) for the poly(I,C)-treated cells. This confirms that the amount of freely available hyaluronan, as a result of poly(I,C) treatment, is only a fraction (29%) of the total produced by the cell. Thus, 71% of the hyaluronan produced by poly(I,C)-treated MASM cells is masked. These data also confirm that essentially all of the hyaluronan, produced by the MASM cells in response to tunicamycin, is freely available for leukocyte adhesion.

*Independent and Additive Effects of Poly(I,C) and Tunicamycin*—Induction of the poly(I,C)-mediated interferon pathways and ER stress, in the same cell, more closely resembles viral infection than either of these alone. Fig. 9 shows the results of an experiment to determine the effect of combining tunicamycin and poly(I,C) treatments. Pre-confluent MASM cell cultures were treated under standard conditions (18 h, 5% FBS) with tunicamycin and poly(I,C), at a dose known to induce maximum hyaluronan-mediated leukocyte adhesion (*plateau doses*; *white bars* of Fig. 9; 5 and 10 $\mu$g/ml, respectively) and a dose inducing leukocyte adhesion at about half of the maximum response (*mid-plateau dose*; *gray bars* of Fig. 9; 0.1 and 0.5 $\mu$g/ml, respectively). Hyaluronan-mediated leukocyte adhesion for the combination was partially, but not completely, additive ($a + b \neq c$; 28 and 21% increase from *TUN* and *PIC*, respectively; $p < 0.002$–$0.0002$) at the plateau doses and slightly more than additive at the mid-plateau doses ($a' + b' = c'$; 50 and 63% increase from *TUN* and *PIC* respectively; $p < 0.0001$) (Fig. 9*A*). Similarly, the amount of hyaluronan in the cell layer, for the combination treatments, was almost completely additive ($a' + b' = c'$; 50 and 43% increase from *TUN* and *PIC*, respectively; $p < 0.02$–$0.008$) when comparing the combined treatments with the individual treatments at the mid-plateau doses (Fig. 9*C*). In contrast, the amount of hyaluronan in the cell layer at the plateau doses was not additive ($a + b \neq c$) for the combination treatments but was actually lower (45%; $p < 0.002$) than poly(I,C) alone, although higher (48%; $p < 0.0001$) than tunicamycin alone. The observation that poly(I,C) and tunicamycin induce independent, yet additive, hyaluronan production and hyaluronan mediated leukocyte adhesion implies that these two toxins function in different, but related, cellular pathways.

From the confluency data (Fig. 8), we learned that leukocyte binding does not show linear proportionality to the amount of hyaluronan on the cell surface. This was probably caused by masking the available surface hyaluronan for binding. For example, a thicker coat of hyaluronan could bind the same number of leukocytes as a thinner coat if they both had the same amount of surface area hyaluronan available for binding. Thus, in Fig. 9, greater leukocyte binding from less hyaluronan (as observed for the combined treatments at plateau doses) could be explained if a thinner coat of surface hyaluronan was more evenly distributed between a greater number of cells. This could happen if a portion of the MASM cells responded to one of the two treatments better than the other.

*Hyaluronan Size Determination from MASM Cells Treated with Poly(I,C) or Tunicamycin*—We treated MASM cells with poly(I,C) (10 $\mu$g/ml) or tunicamycin (5 $\mu$g/ml) under standard conditions (18 h, 5% FBS). We purified the hyaluronan (and other glycosaminoglycans) through a series of enzymatic digestions (proteinase, nuclease, and glycosidase) and precipitations (as fully described in "Experimental Procedures"), analyzing the extracts by agarose gel electrophoresis (Fig. 10). This resulted in a blue, high molecular weight (HMW) smear (1500–4000 kDa) that was confirmed as hyaluronan by pre-digestion with *Streptomyces* hyaluronidase (Fig. 10*A*, *lanes 4, 6,* and *8*). The molecular weight range was similar in each of the treatment conditions (untreated (*NT*), tunicamycin, and poly(I,C); *lanes 3, 5,* and *7*, respectively). The smears below 27 kDa are likely heparan sulfate (Fig. 10*A*, *yellow/brown*) and chondroitin sulfate (*purple*).[4] We were surprised that although the hyaluronan is present as a 1500–4000-kDa smear, a significant amount was present in a fairly defined band at about 4000 kDa. Because this

[4] M. Lauer, A. Wang, and V. C. Hascall, personal observations.

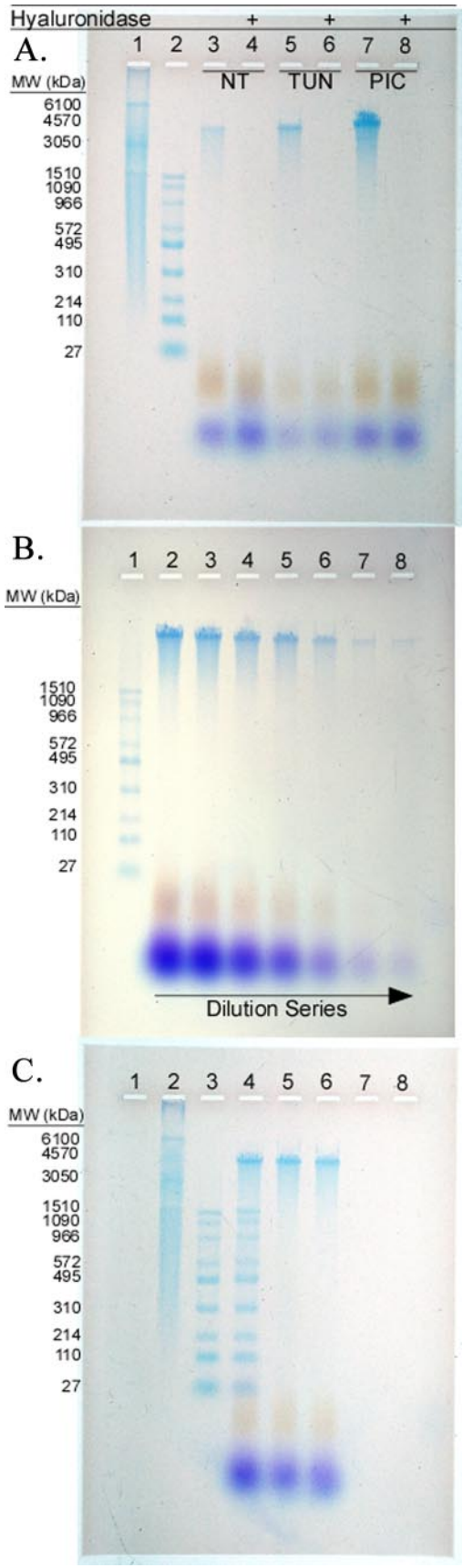


FIGURE 10. **Hyaluronan size determination from MASM cells treated with poly(I,C) or tunicamycin.** Hyaluronan size determination by agarose gel electrophoresis was done on MASM cells either untreated (*NT*; *A*, *lanes 3* and *4*), treated with tunicamycin (*TUN*; *lanes 5* and *6*), or treated with poly(I,C) (*PIC*; *lanes 7* and *8*). Purified hyaluronan from these samples was digested with (*lanes 4, 6,* and *8*) or without (*lanes 3, 5,* and *7*) *Streptomyces* hyaluronidase to confirm purity. Hyaluronan molecular weight (*MW*) standards are in *lanes 1* and *2*. The same is true for *C*, but *B* only has the lower molecular weight standards (*lane 1*). Please note that the HMW standards (*lane 1*) give three distinct bands from the nine bands of the lower molecular weight standards (*lane 2*), despite the unfortunate smearing. Hyaluronan is stained *blue*, and the *yellow/brown* and *purple* staining are most likely heparan sulfate and chondroitin sulfate, respectively (personal observations, see Footnote 4). *A*, 10 $\mu$l of each sample was added to each well, and this volume represented one-half of the total cellular extract from a single 175-cm$^2$ culturing flask. *B*, we diluted a MASM sample representing hyaluronan derived after poly(I,C) treatment (similar to the sample of *A*, *lane 7*, but yet a separate sample) in the following way: 100, 80, 60, 40, 20, 10, and 5% (*lanes 2–8,* respectively). The volume of each of these samples was adjusted to 10 $\mu$l with TAE so that the actual concentration and volume of the samples were directly related. The diluted samples were incubated at 4 °C overnight and electrophoresed the next day (*B*). *C*, an identical aliquot from *B, lane 5,* was mixed with the lower molecular weight standard of *lane 3* (10 $\mu$l final volume) and incubated at 4 °C overnight (*lane 4*). Furthermore, two additional identical aliquots from *B, lane 5,* were lyophilized and rehydrated in either 10 $\mu$l of 100 mM ammonium acetate, pH 7.0 (*lane 5*), or 10 $\mu$l of 4 M guanidine, 2% CHAPS, and 0.05 M Tris-HCl, pH 7.0 (*lane 6*), and incubated overnight at 4 °C and precipitated with 40 $\mu$l of ethanol the next day. After centrifugation, the pellets were resuspended in 10 $\mu$l of TAE, incubated overnight at 4 °C, and electrophoresed the next day. *Lanes 1, 7,* and *8* of *C* are blank. The experiment in *A* was repeated >3 times in different experiments with similar results.

phenomenon could be caused by the aggregation of multiple hyaluronan strands, we made serial dilutions from a separate aliquot of the poly(I,C)-induced hyaluronan to determine whether this unusual HMW band might be related to the concentration of hyaluronan in solution (Fig. 10*B*). Within the range of detection, diluted hyaluronan did not show a dissolution of the HMW band. Another possible cause for hyaluronan aggregation might be that the ionic conditions (TAE buffer and any other salts that might not have been removed by ethanol precipitation) of the samples induce aggregation. But when a hyaluronan molecular weight standard was added to a hyaluronan extract from poly(I,C)-treated MASM cells (Fig. 10*C*, *lane 4*), no differences in band migration occurred, indicating that the ionic conditions of the sample were not responsible for the high molecular weight band. Finally, we compared hyaluronan from poly(I,C)-induced MASM cells, purified under routine conditions (Fig. 10*C*, *lane 5*), with identical hyaluronan that had been exposed to 4 M guanidine, 2% CHAPS, and 0.05 M Tris-HCl, pH 7.0, as a means to disassociate any potential hyaluronan aggregates (*lane 6*). The failure of any of these approaches to disrupt the HMW (~4000 kDa) hyaluronan band confirms that this band represents the actual molecular weight of unassociated hyaluronan strands.

## DISCUSSION

In this paper, we described the hyaluronan-mediated response of MASM cells to poly(I,C) and tunicamycin, which are models that mimic viral infection and ER stress relevant to airway inflammation associated with asthma (23, 27, 38, 40, 41).

Our results demonstrate that MASM cells respond to both poly(I,C) and tunicamycin to produce a leukocyte-adhesive hyaluronan matrix, but accomplish this by different cellular pathways. At all cell densities studied, MASM cells initiate synthesis of the hyaluronan matrix immediately after the addition of poly(I,C). This matrix accumulates linearly for

10–12 h, resulting in a 7–9-fold increase in the amount of cell-associated hyaluronan matrix. In contrast, the response of the MASM cells to tunicamycin depends on cell density, with pre-confluent densities responding most effectively. Tunicamycin-induced hyaluronan accumulation is nearly linear for 10–12 h, although the matrix accumulation is much less (~2-fold at most). In both treatments, the normal pathway for synthesis and secretion of hyaluronan into the medium is not significantly altered, which indicates that the hyaluronan response to poly(I,C) and tunicamycin is completely associated with the cell matrix.

Although U937 leukocytes adhere to the hyaluronan matrix produced by both reagents, the number bound per hyaluronan in the matrix is much higher for tunicamycin-treated MASM cell cultures. This implies that the more robust cable structures produced by poly(I,C)-treated MASM cells mask many sites that remain accessible in the more disperse hyaluronan matrix initiated by tunicamycin. These results are consistent with the observation that there is no difference between the numbers of leukocytes that bind to tunicamycin-treated MASM cells after hyaluronidase treatment compared with the number that remained bound when the hyaluronidase treatment followed the initial adhesion. In contrast, hyaluronidase digestion before leukocyte adhesion in poly(I,C)-treated MASM cultures increased the number of bound leukocytes (probably via VCAM), indicating that many of the sites on the cell surfaces were masked by the more copious hyaluronan matrix synthesized in response to poly(I,C).

Additionally, poly(I,C) treatment of MASM cells, in addition to inducing hyaluronan-mediated leukocyte adhesion, also induces the expression of VCAM-1, which promotes hyaluronan-independent leukocyte adhesion. In contrast, tunicamycin did not induce VCAM-1-mediated leukocyte adhesion, but promoted the up-regulation of chaperones in the ER (KDEL staining, see Fig. 7), which was not induced in poly(I,C)-treated cells.

Synthesis of the abnormal hyaluronan matrix by MASM cells in response to poly(I,C) also depends on serum concentration, with much less of this matrix formed in its absence. This indicates that an as yet unknown factor in serum is necessary. However, heavy chains from the inter-$\alpha$-inhibitor, a likely candidate based upon previous studies (42, 43), are not involved as shown in our accompanying article (59). In contrast, synthesis and secretion of hyaluronan by the normal pathway are still present in the absence of serum. Interestingly, leukocyte binding that is independent of hyaluronan is highest when the MASM cells are incubated in the absence of serum (Fig. 3*C*).

We were surprised to see that the size of hyaluronan by MASM cells treated with poly(I,C) or tunicamycin was not different from the hyaluronan made by untreated cells. We were also surprised that much of the hyaluronan produced under each of these conditions occurs as a well defined ~4000-kDa band. In addition to this defined band, the hyaluronan we were able to detect appeared as a smear, ranging from 1500 to 4000 kDa. It is interesting that this smear only occurs *below* the 4000-kDa band, implying that the hyaluronan synthases from the MASM cells shut off hyaluronan synthesis beyond 4000 kDa, while permitting a certain amount of synthetic leeway between 1500 and 4000 kDa.

Previous studies showed that the synthesis of the abnormal hyaluronan matrix is initiated and continues when aortic smooth muscle cells are treated with cycloheximide (37), which rapidly inhibits all protein synthesis. These results suggest that the mechanism for initiating and sustaining synthesis of the abnormal hyaluronan matrix is latent within the cells and only requires activation in response to various forms of stress by possibly phosphorylating and dephosphorylating different kinases that can regulate this pathway. There is indirect evidence demonstrating that the activity of HAS isoforms can be rapidly modulated by protein kinase C, protein kinase A, and/or by a calcium-dependent protein kinase, and there is direct evidence that phosphorylation of human HAS3 can be enhanced by a variety of physiological effectors (44). One recent study reported that phosphorylation/activation of HAS *in vivo* by ErbB2 tyrosine kinase and ERK (extracellular signal-related kinase) activities leads to hyaluronan production and size modification (45). It is also possible that activation of PKR (double-stranded RNA-dependent protein kinase) by poly(I,C) and PERK (ER resident transmembrane protein kinase) by tunicamycin both converge on the pathway of eIF2 phosphorylation. However, in a recent study, tunicamycin was shown to activate PKR, which participates in the cell death induced by ER stress (46). The cross-talk between these two pathways regulating protein synthesis by eIF2$\alpha$ phosphorylation and protein degradation may have a significant impact in diseases such as viral infection, diabetes, and cancer (47).

The abnormal hyaluronan matrix increases in proportion to cell number with poly(I,C) treatment, although it decreases with increased cell number with tunicamycin treatment. This may indicate that pre-confluent MASM cells are synthesizing more protein in their proliferative phase and are therefore more sensitive to ER stress. If this is the case, the poly(I,C) response appears to be independent of the load of protein synthesis.

There are at least three cellular pathways that can initiate the synthesis of the abnormal hyaluronan matrix. In addition to the viral and ER stress responses, mesangial cells stimulated to divide in hyperglycemic medium produce a leukocyte-adhesive matrix (48). Furthermore, recent studies have shown that 3T3-L1 cells that are differentiated to adipocytes in hyperglycemic medium also produce this matrix (49). ER stress may also link obesity and insulin resistance in type 2 diabetes (50). This report showed that high fat feeding and obesity induce ER stress in liver, which suppresses insulin signaling via c-Jun N-terminal kinase activation.

Several studies indicate that leukocytes adhere to certain hyaluronan matrices synthesized by cells subjected to various stress responses, but not others, such as hyaluronan coats made by cells normally (51). For example, lymphocytes interact with the abnormal hyaluronan matrix produced by venules and endothelial cells produced in graft *versus* host disease, but do not do so to the adjacent normal hyaluronan matrix in the papillary dermis (52). Kidney renal tubule endothelial cell cultures stimulated with either BMP-7 or interleukin-1$\beta$ increase hyaluronan synthesis (53). However, lymphocytes only adhere to

the hyaluronan matrix produced in response to BMP-7. This suggests that the increase in hyaluronan synthesis by interleukin-1$\beta$ reflects stimulation of the normal hyaluronan synthesis pathway. Lymphocytes adhere much more avidly to hyaluronan with covalently bound heavy chains of inter-$\alpha$-inhibitor than to unsubstituted hyaluronan (54). All of these results indicate that hyaluronan matrices produced in response to stress contain structural information that inflammatory cells can recognize.

Under normal physiological conditions, hyaluronan is cleared from connective tissues through the lymphatics (55) or by the resident cells (56, 57). In contrast, under some pathological conditions, as in asthmatic airways, the abnormal hyaluronan matrix is removed by the leukocytes/macrophages that enter the tissue. Degradation of the abnormal matrix by these cells could release hyaluronan fragments, which are now considered "danger signals" in initiating host responses to the inflammatory process and likely participate in determining the extent of the response (58). Overproduction of the matrix or over-reaction by inflammatory cells to this matrix may contribute to the inflammatory flares that are typical of asthmatic patients.

## REFERENCES


1. Bousquet, J., Jeffery, P. K., Busse, W. W., Johnson, M., and Vignola, A. M. (2000) *Am. J. Respir. Crit. Care Med.* **161,** 1720–1745
2. Homer, R. J., and Elias, J. A. (2000) *Clin. Chest Med.* **21,** 331–343
3. Hakonarson, H., Maskeri, N., Carter, C., Hodinka, R. L., Campbell, D., and Grunstein, M. M. (1998) *J. Clin. Investig.* **102,** 1732–1741
4. Phipps, S., Benyahia, F., Ou, T. T., Barkans, J., Robinson, D. S., and Kay, A. B. (2004) *Am. J. Respir. Cell Mol. Biol.* **31,** 626–632
5. Alcorn, J. F., Rinaldi, L. M., Jaffe, E. F., van Loon, M., Bates, J. H. T., Janssen-Heininger, Y. M. W., and Irvin, C. G. (2007) *Am. J. Respir. Crit. Care Med.* **176,** 974–982
6. Park, J. W., Taube, C., Swasey, C., Kodama, T., Joetham, A., Balhorn, A., Takeda, K., Miyahara, N., Allen, C. B., Dakhama, A., Kim, S. H., Dinarello, C. A., and Gelfand, E. W. (2004) *Am. J. Respir. Cell Mol. Biol.* **30,** 830–836
7. Hirst, S. J., Twort, C. H., and Lee, T. H. (2000) *Am. J. Respir. Cell Mol. Biol.* **23,** 335–344
8. Mukhopadhyay, D., Lauer, M., de la Motte, C. A., Erzurum, S. C., Fulop, C., and Hascall, V. C. (2006) *Matrix Biol.* **25,** S94
9. Forteza, R., Lieb, T., Aoki, T., Savani, R. C., Conner, G. E., and Salathe, M. (2001) *FASEB J.* **15,** 2179–2186
10. Ludwig, M. S. (2007) *J. Appl. Physiol.* **103,** 735–736
11. Sahu, S., and Lynn, W. S. (1978) *Biochem. J.* **173,** 565–568
12. Coyle, A. J., Bertrand, C., Tsuyuki, S., Pircher, H., Walti, S., Le, G. G., and Erard, F. (1996) *Ann. N. Y. Acad. Sci.* **796,** 97–103
13. Ehlenfield, D. R., Cameron, K., and Welliver, R. C. (2000) *Pediatrics* **105,** 79–83
14. Hamid, Q., Tulic', M. K., Liu, M. C., and Mogbel, R. (2003) *J. Allergy Clin. Immunol.* **111,** S5–S17
15. Robinson, D. S. (2004) *J. Allergy Clin. Immunol.* **114,** 58–65
16. Hascall, V. C., and Laurent, T. C. (1997) in *Science of Hyaluronan Today* (Hascall, V. C., and Yanagishita, M., eds) Seikagaku Corp., Tokyo, Japan
17. Weigel, P. H., Hascall, V. C., and Tammi, M. (1997) *J. Biol. Chem.* **272,** 13997–14000
18. Day, A. J. (1999) *Biochem. Soc. Trans.* **27,** 115–121
19. Toole, B. P. (1990) *Curr. Opin. Cell Biol.* **2,** 839–844
20. Katoh, S., Matsumoto, N., Kawakita, K., Tominaga, A., Kincade, P. W., and Matsukura, S. (2003) *J. Clin. Investig.* **111,** 1563–1570
21. Lazaar, A. L., Albelda, S. M., Pilewski, J. M., Brennan, B., Pure, E., and Panettieri, R. A., Jr. (1994) *J. Exp. Med.* **180,** 807–816
22. Lesley, J., Hyman, R., and Kincade, P. W. (1993) *Adv. Immunol.* **54,** 271–335
23. An, S. S., Bai, T. R., Bates, J. H. T., Black, J. L., Brown, R. H., Brusasco, V., Chitano, P., Deng, L., Dowell, M., Eidelman, D. H., Fabry, B., Fairbank, N. J., Ford, L. E., Fredberg, J. J., Gerthoffer, W. T., Gilbert, S. H., Gosens, R., Gunst, S. J., Halayko, A. J., Ingram, R. H., Irvin, C. G., James, A. L., Janssen, L. J., King, G. G., Knight, D. A., Lauzon, A. M., Lakser, O. J., Ludwig, M. S., Lutchen, K. R., Maksym, G. N., Martin, J. G., Mauad, T., McParland, B. E., Mijailovich, S. M., Mitchell, H. W., Mitchell, R. W., Mitzner, W., Murphy, T. M., Pare, P. D., Pellegrino, R., Sanderson, M. J., Schellenberg, R. R., Seow, C. Y., Silveira, P. S. P., Smith, P. G., Solway, J., Stephens, N. L., Sterk, P. J., Stewart, A. G., Tang, D. D., Tepper, R. S., Tran, T., and Wang, L. (2007) *Eur. Respir. J.* **29,** 834–860
24. Hascall, V. C., Majors, A. K., de la Motte, C. A., Evanko, S. P., Wang, A. M., Drazba, J. A., Strong, S. A., and Wight, T. N. (2004) *Biochim. Biophys.* **1673,** 3–12
25. Roberts, C. R. (1995) *Chest* **107,** S111–S117
26. Bousquet, J., Chanez, P., Lacoste, J. Y., Enander, I., Venge, P., Peterson, C., Ahlstedt, S., Michel, F. B., and Godard, P. (1991) *J. Allergy Clin. Immunol.* **88,** 649–660
27. Teder, P., Vandivier, R. W., Jiang, D., Liang, J., Cohn, L., Pure, E., Henson, P. M., and Noble, P. W. (2002) *Science* **296,** 155–158
28. Niimi, K., Asano, K., Shiraishi, Y., Nakajima, T., Wakaki, M., Kagyo, J., Takihara, T., Suzuki, Y., Fukunaga, K., Shiomi, T., Oguma, T., Sayama, K., Yamaguchi, K., Natori, Y., Matsumoto, M., Seya, T., Yamaya, M., and Ishizaka, A. (2007) *J. Immunol.* **178,** 489–495
29. Oliver, B., Johnston, S., Baraket, M., Burgess, J., King, N., Roth, M., Lim, S., and Black, J. (2006) *Respir. Res.* **7,** 71
30. Corne, J. M., Marshall, C., Smith, S., Schreiber, J., Sanderson, G., Holgate, S. T., and Johnston, S. L. (2002) *Lancet* **359,** 831–834
31. Grissell, T. V., Powell, H., Shafren, D. R., Boyle, M. J., Hensley, M. J., Jones, P. D., Whitehead, B. F., and Gibson, P. G. (2005) *Am. J. Respir. Crit. Care Med.* **172,** 433–439
32. Papadopoulos, N. G., Bates, P. J., Bardin, P. G., Papi, A., Leir, S. H., Fraenkel, D. J., Meyer, J., Lackie, P. M., Sanderson, G., Holgate, S. T., and Johnston, S. L. (2000) *J. Infect. Dis.* **181,** 1875–1884
33. Braunstahl, G. J., Fokkens, W. J., Overbeek, S. E., KleinJan, A., Hoogsteden, H. C., and Prins, J. B. (2003) *Clin. Exp. Allergy* **33,** 579–587
34. Isler, J. A., Skalet, A. H., and Alwine, J. C. (2005) *J. Virol.* **79,** 6890–6899
35. Mulvey, M., Arias, C., and Mohr, I. (2006) *J. Virol.* **80,** 7354–7363
36. de la Motte, C. A., Hascall, V. C., Calabro, A., Yen-Lieberman, B., and Strong, S. A. (1999) *J. Biol. Chem.* **274,** 30747–30755
37. Majors, A. K., Austin, R. C., de la Motte, C. A., Pyeritz, R. E., Hascall, V. C., Kessler, S. P., Sen, G., and Strong, S. A. (2003) *J. Biol. Chem.* **278,** 47223–47231
38. Lee, E. S., Yoon, C. H., Kim, Y. S., and Bae, Y. S. (2007) *FEBS Lett.* **581,** 4325–4332
39. Calabro, A., Hascall, V. C., and Midura, R. J. (2000) *Glycobiology* **10,** 283–293
40. Robinson, D. S., North, J., Zeibecoglou, K., Ying, S., Meng, Q., Rankin, S., Hamid, Q., Tavernier, J., and Kay, A. B. (1999) *Int. Arch. Allergy Immunol.* **118,** 98–100
41. Roberts, C. R., and Burke, A. K. (1998) *Can. Respir. J.* **5,** 48–50
42. de la Motte, C. A., Hascall, V. C., Drazba, J., Bandyopadhyay, S. K., and Strong, S. A. (2003) *Am. J. Pathol.* **163,** 121–133
43. Selbi, W., de la Motte, C. A., Hascall, V. C., Day, A. J., Bowen, T., and Phillips, A. O. (2006) *Kidney Int.* **70,** 1287–1295
44. Goentzel, B. J., Weigel, P. H., and Steinberg, R. A. (2006) *Biochem. J.* **396,** 347–354
45. Bourguignon, L. Y. W., Gilad, E., and Peyrollier, K. (2007) *J. Biol. Chem.* **282,** 19426–19441
46. Shimazawa, M., Ito, Y., Inokuchi, Y., and Hara, H. (2007) *Investig. Ophthalmol. Vis. Sci.* **48,** 3729–3736
47. Saavalainen, K., Tammi, M. I., Bowen, T., Schmitz, M. L., and Carlberg, C. (2007) *J. Biol. Chem.* **282,** 11530–11539
48. Wang, A., and Hascall, V. C. (2004) *J. Biol. Chem.* **279,** 10279–10285
49. Han, C. Y., Subramanian, S., Chan, C. K., Omer, M., Chiba, T., Wight, T. N., and Chait, A. (2007) *Diabetes* **56,** 2260–2273
50. Eizirik, D. L., Cardozo, A. K., and Cnop, M. (2008) *Endocr. Rev.* **29,** 42–61
51. Jokela, T. A., Lindgren, A., Rilla, K., Maytin, E., Hascall, V. C., Tammi, R. H., and Tammi, M. I. (2008) *Connect. Tissue Res.* **49,** 115–119

52. Milinkovic, M., Antin, J. H., Hergrueter, C. A., Underhill, C. B., and Sackstein, R. (2004) *Blood* **103,** 740–742
53. Selbi, W., Day, A. J., Rugg, M. S., Fulop, C., de la Motte, C. A., Bowen, T., Hascall, V. C., and Phillips, A. O. (2006) *J. Am. Soc. Nephrol.* **17,** 1553–1567
54. Zhao, M., Yoneda, M., Ohashi, Y., Kurono, S., Iwata, H., Ohnuki, Y., and Kimata, K. (1995) *J. Biol. Chem.* **270,** 26657–26663
55. Fraser, J. R., Kimpton, W. G., Laurent, T. C., Cahill, R. N., and Vakakis, N. (1988) *Biochem. J.* **256,** 153–158
56. Laurent, U. B., Dahl, L. B., and Reed, R. K. (1991) *Exp. Physiol.* **76,** 695–703
57. Laurent, U. B., Fraser, J. R., Engstrom-Laurent, A., Reed, R. K., Dahl, L. B., and Laurent, T. C. (1992) *Matrix* **12,** 130–136
58. Scheibner, K. A., Lutz, M. A., Boodoo, S., Fenton, M. J., Powell, J. D., and Horton, M. R. (2006) *J. Immunol.* **177,** 1272–1281
59. Lauer, M. E., Fulop, C., Mukhopadhyay, D., Comhair, S., Erzurum, S. C., and Hascall, V. C. (2009) *J. Biol. Chem.* **284,** 5313–5321